

General Disclaimer

One or more of the Following Statements may affect this Document

- This document has been reproduced from the best copy furnished by the organizational source. It is being released in the interest of making available as much information as possible.
- This document may contain data, which exceeds the sheet parameters. It was furnished in this condition by the organizational source and is the best copy available.
- This document may contain tone-on-tone or color graphs, charts and/or pictures, which have been reproduced in black and white.
- This document is paginated as submitted by the original source.
- Portions of this document are not fully legible due to the historical nature of some of the material. However, it is the best reproduction available from the original submission.

NASA TECHNICAL MEMORANDUM

NASA TM-76917

THE NH BANDS AT λ 3360

G. W. Funke

Translation of "Die NH Banden bei λ 3360." Zeitschrift fuer Physik,
Vol. 96, 1935, pp. 787-798.

(NASA-TM-76917) THE NH BANDS AT LAMBDA 3360
(National Aeronautics and Space
Administration) 14 p HC A02/MF A01 CSCL 20K

N82-28185

Uncclas
G3/76 28280

NATIONAL AERONAUTICS AND SPACE ADMINISTRATION
WASHINGTON, D.C. 20546 MARCH 1982

STANDARD TITLE PAGE

1. Report No. NASA TM-76917	2. Government Accession No.	3. Recipient's Catalog No.	
4. Title and Subtitle THE NH BANDS AT λ 3360		5. Report Date March 1982	
		6. Performing Organization Code	
7. Author(s) G. W. Funke		8. Performing Organization Report No.	
		10. Work Unit No.	
9. Performing Organization Name and Address Leo Kanner Associates Redwood City, California 94063		11. Contract or Grant No. NASW-3541	
12. Sponsoring Agency Name and Address National Aeronautics and Space Administration Washington, DC 20546		13. Type of Report and Period Covered Translation	
14. Sponsoring Agency Code			
15. Supplementary Notes Translation of "Die NH Banden bei λ 3360," Zeitschrift fuer Physik, Vol. 96, 1935, pp. 787-798.			
16. Abstract A detailed analysis of the bands at λ 3360 and 3370 is given; their λ and spin splitting as well as a widening effect which can be observed at these bands are described. The bands form the 0-0 and 1-1 transitions of a $^3\Pi$ and $^3\Sigma$ system. The recordings were made at a dispersion of 0.42 Å/mm.			
17. Key Words (Selected by Author(s))		18. Distribution Statement Unclassified - Unlimited	
19. Security Classif. (of this report) Unclassified	20. Security Classif. (of this page) Unclassified	21. No. of Pages 13	22. Price

THE NH BANDS AT λ 3360

G.W. Funke

Stockholm

A detailed analysis of the bands at λ 3360 and 3370 is given; their A and spin splitting as well as a widening effect which can be observed at these bands are described. The bands form the 0-0 and 1-1 transitions of a ^3II and $^3\Sigma$ system. The recordings were made at a dispersion of 0.42 Å/mm. /787*

The band spectrum of NH at $\lambda\lambda$ 3360 and 3370 has been the object of repeated studies¹⁾. Hulthen and Nakamura found that they are the 0-0 and 1-1 bands of a ^3II and $^3\Sigma$ system, it has been proved to be difficult, however, to carry out a detailed analysis of the spectrum, partly because of the fact that the B-values in ^3II and $^3\Sigma$ are close and similar resulting in Q-branches forming dense line accumulations which are hard to dissolve. Additionally, the intensive 0-0 band of the second positive nitrogen group has an edge with a corner cutting toward violet at λ 3371. Their lines superimpose over the already dense conglomerate of the NH bands thus increasing the difficulty of analyzing it.

Experiments

In order to start with this system at all, two conditions have to be fulfilled; the disturbing nitrogen spectrum has to be removed and the recordings have to be made with a spectrograph of as large as possible resolution. One way to remove the nitrogen spectrum is by using an illuminating gas ammonia flame or an oxygen ammonia flame as

*Numbers in the margin indicate pagination in the foreign text.

1) A. Fowler u. CL. Gregory, Phil. Trans. Roz. Soc. London (A) 218, 251, 1919; K. Gleu, ZS. F. Phys. 38, 176, 1926; E. Hulthen u. S. Nakamara, Nature 119, 235, 1927; R.W.B. Pearse, Phus. Rev. 37, 1712, 1931; H. Batsch, Ann.d.Phys. 18, 1933; Ritzmann, Dissertation, Breslau, 1934

light source; the obtained spectrum, however, is too dull, it cannot be received in a large spectrograph. This is why we used a vacuum light arc which can also be used as pressure arc. In order to find the most favorable conditions, experiments with various nitrogen-water mixtures were at first carried out without, however, receiving satisfactory results. It could be shown, however, that the nitrogen bands become weaker when the pressure was increased. Experiments with ammonia had better results, and if the gas flows and pressure is kept over 2 atm, the spectrum is completely clean. The increased pressure has, however, a new disadvantage; the line width is increased by the pressure. The plate best suited for the analysis was consequently exposed at a pressure of 1000 mm.

/788

Based upon the above-mentioned experiments, the recording was then made in the following manner: a pressure arc with especially forceful water cooling was used as light source which could be loaded up to 15 amp at least. The light arc burned between two tungsten electrodes which do not have a disturbing atomic spectrum under these conditions. The voltage was 440 V. We might mention that this light arc has an extraordinary appearance inasmuch as it contracts to a thin thread when the pressure is increased; under the influence of the field of both electrodes this thread curves outward in a loop. If pressure or current are increased too much, this loop curves outward until it breaks and the arc becomes extinct. Under pressures and currents when the arc burned without becoming extinct, the thin lighting thread oscillated to and fro; this is why the complete arc was put on wheels, so that the picture of the thin light arc could be fixed to the slit during the exposure. Gas was introduced into the pressure arc from a tank with liquid ammonia; from the pressure arc it was led into water where the part of the ammonia which was not decomposed by the light arc was absorbed. In the experiments with a pressure lower than air pressure in the arc, a water jet pump was used to suck the gas from the arc. Simultaneously, it served as pump and absorption medium for NH_3 and it is the simplest feasible setup in a case like this without disturbing OH bands.

In order to obtain the necessary resolution, the recordings were made in the 4th order of our large concave grid with a dispersion of 0.42 \AA in this range.

Analysis

A complete $^3\text{II} - ^3\Sigma$ band should consist of 27 branches as is the case with the hydride of the following element in the same column of the periodic system, i.e. PH ²⁾. It cannot be expected that all these branches exist for the NH molecule because the distance of the components in ^3II is 10 or 20 cm^{-1} and $^3\Sigma$ consequently belongs to Hund's coupling case. 9 main branches, one P and one R satellite were here observed. The other S side branches which should be expected if ^3II is close to case b) obviously are too weak to show on the plate. The Q satellites cannot be separated from the compressed mass of other lines. The P and R satellites are too weak to be detected on the plates of the 4th order: they were measured on an overexposed plate of the 1st order, i.e., with a dispersion of about 1.7 \AA/mm . It can possibly be assumed that these weak branches are caused by the nitrogen isotope N^{15} ; this, however, is impossible since $\rho-1$ and $\rho-2$ are negative and $r'_1 - r = (\rho-1) r$, or $r'_r - r = (\rho^2-1) r$, would show the isotope lines at the red side of the main lines of R_2 . The P satellite is in the right position of P_2 , with increasing K, the splitting, however, is decreased instead of increased, as it should be if it represented a rotation isotopic effect. The nuclear vibration effect is not considered at all since it is very small due to the equality of ω' and ω'' .

R_1 , R_2 , R_3 and Q_1 form edges which have corner cutting toward red. Q_2 , Q_3 and the P branches, however, do not form edges. Based on these facts the peculiar structure of this band system can now be understood. The corner cutting at the short wavelength side of the maximum is due to the Q_2 and Q_3 branches and especially to the initially decreasing distance between the various lines in Q_3 from red toward shorter wavelengths until a distance minimum of $K=9$ is

²⁾ R.W.B. Pearce, Proc. Roy. Soc. London (A) 129, 328, 1930

reached; it then increases again. For the line distance within the P branches the same is true as for Q₃.

The term diagram represented in Fig. 1 cannot be deduced in all details from facts known about NH; a comparison with other similar, known spectrums has to be used too. Already Mulliken stated that the $^3\Sigma$ state has to be termed $^3\Sigma$, and this means that all levels with even K are negative. Levels with J = K + 1 are termed F₁, those with J = K are termed F₂ and those with J = K - 1 are F₃. The numbering of the individual lines was carried out after K in the final stage.

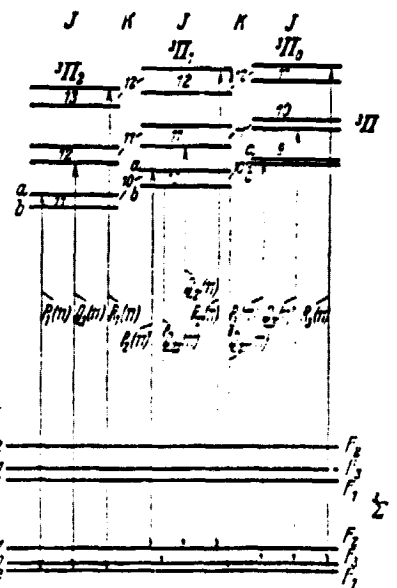


Fig. 1. Term Diagram

The excited stage

Based on van Vleck's studies, Mulliken gave a general term formula for case b), but since not all functions in it are known for ^3II and since the function referring to the Λ splitting additionally does not conform well with theory in this case, we only use the formula

$$F(K) = B_v K(K+1) + D_v K^2(K+1)^2 + F_v K^3(K+1)^3$$

which represents the term without considering Λ and spin splitting. Calculating the constants, only values of $^3\Pi_1$ were used and a mean value between $\Delta_1 F_a$ and $\Delta_1 F_b$ was calculated by the following equation:³⁾

$$\frac{Q(K) - P(K) + R(K-1) - Q(K-1)}{2} = \Delta_1 F(K)$$

$$= F(K) - F(K-1) = 2B_v K + 4D_v K^2 + F_v K^3(6K^2 + 2).$$

³⁾This assumption is in a way arbitrary, but it should be the most suitable one until a detailed theory on Λ splitting in ^3II is found.

ORIGINAL PAGE IS
OF POOR QUALITY

Table 1. Table of band lines. 0-0

<i>K</i>	<i>E</i>	<i>P₃</i>	<i>Q₃</i>	<i>E₄</i>	<i>P₂</i>	<i>Q₂</i>	<i>R₂</i>	<i>P₁</i>	<i>Q₁</i>	<i>R₁</i>	<i>P_{Q₂1}</i>	<i>R_{Q₂1}</i>
0				29813.20							29772.58	
1				873.10							809.84	
2				902.89							816.17	
3		29782.90		902.69	29634.28	29762.26	925.21				881.18	
4		777.38		902.69	29634.28	29762.26	925.21				915.22	
5	29609.71	773.43		902.96	601.20	761.46	956.66	29688.46			948.34	
6	575.32	770.35		993.36	568.11	760.69	987.90	658.07			981.04	
7	544.78	768.52	30023.69	635.55	759.71	30018.96	627.48			30018.08	29536.68	30020.09
8	508.82	766.57	0.3.75	603.43	758.61	019.57	496.69			044.72	504.65	050.80
9	476.32	761.98	083.51	471.71	757.70	079.84	466.00			075.70	472.72	081.05
10	444.24	763.20	112.76	440.20	756.52	109.47	436.46			105.94	441.23	110.66
11	412.70	761.46	111.56	409.08	755.48	138.68	406.06			135.69	410.35	140.03
12	381.38	759.71	169.64	378.28	753.92	167.16	374.84	29761.43		164.61	379.28	
13	350.52	757.70	197.11	347.85	752.3	191.89	344.83	750.3		192.72		
14	320.03	755.48	223.76	317.61	750.45	221.88	315.15	749.0		220.10		
15	289.87	753.3	249.68	287.78	748.41	248.02	285.64	747.27		246.53		
16	260.06	750.8	274.51	258.19	746.20	273.22	266.60	745.31		272.02		
17	230.53	747.8	298.51	228.94	743.55	297.37	227.64	742.81		296.41		
18	201.33	744.49	321.30	199.96	740.63	320.36	198.92	740.1		319.75		
19	172.36	740.63	342.99	171.28	737.03	342.15	170.43	737.03		341.79		
20	143.72	737.03	363.32	142.77	733.10	362.58	142.23	733.10		362.68		
21	115.27	732.17	382.15	114.49	728.74	381.76	114.28	728.74		381.76		
22	86.91	727.10	399.51	86.39	728.73	399.51	86.39	728.97		399.54		
23	658.70	721.29	415.53	658.52	717.99	415.53	658.52	718.44		415.63		
24	630.66	714.73	429.78	630.56	711.62	429.78	630.66	712.80		429.78		
25	602.57	707.42	442.06	602.57	704.41	442.06	602.57	705.19		442.65		
26	28974.50	699.14	452.39	28974.50	696.83	452.39	28974.50			697.21		
27	946.03	689.94		946.03	687.15		946.68			688.28		
28	917.41	679.65		917.41	676.97		918.41			678.08		
29	888.45	668.02		888.45	666.43		889.66					
30	869.06			869.06			860.82					
31	covered			covered			830.23					
32	798.06			798.06			799.47					
33	760.22			760.22			767.61					
34	732.30			732.30			731.62					
35	698.11			698.11			690.92					

ORIGINAL PAGE IS
OF POOR QUALITY

Table 2. Table of banc lines. 1-1

<i>K</i>	<i>P₃</i>	<i>Q₃</i>	<i>R₃</i>	<i>P₂</i>	<i>Q₂</i>	<i>R₂</i>	<i>P₁</i>	<i>Q₁</i>	<i>R₁</i>
1									
2			29777.38						
3		805.07			672.23	796.19			
4	29559.05		832.61	29548.36	669.45	826.06	531.52		29784.01
5	523.44	29676.97	860.41	514.90	666.98	853.85	501.88		814.78
6	489.96	673.68	888.10	481.88	664.83	882.37	471.67		816.46
7	456.15	670.40	916.22	449.53	662.30	910.43	441.23		876.38
8	422.78	666.98	942.15	417.34	659.61	937.74	410.35		904.53
9	389.88	663.43	968.48	385.05	656.57	964.62	379.28		932.69
10	357.25	659.61	994.25	352.96	663.1	990.77	347.85		960.39
11	324.70	655.00	30018.96	320.98	649.4	30016.10	316.71	29646.94	30013.08
12	292.24	651.08	042.99	288.93	645.3	040.33	285.64	643.34	037.58
13	260.06	645.65	066.02	257.02	640.62	063.64	251.02	639.13	061.34
14	227.61	640.62	087.91	225.21	635.59	085.87	222.66	634.28	063.98
15	195.71	634.28	108.60	193.40	629.84	196.82	191.27	628.73	105.20
16	163.60	627.77	128.20	161.58	623.39	126.57	159.84	622.48	125.26
17	131.45	620.35	146.20	129.87	616.07	144.85	128.23	615.65	143.84
18	099.36	612.21	162.91	097.88	608.08	161.68	096.63	608.08	160.85
19	067.02	603.19	177.79	065.81	599.40	176.77	064.90	599.40	176.30
20	034.52	593.27	190.95	033.40	589.71	190.11	033.40	589.71	190.11
21	covered	582.28	202.31	001.05	578.92	201.60	001.05	578.92	201.60
22	28968.83	570.16	211.11	28967.89	567.06	211.11	28967.89	567.06	211.11
23	936.42	566.77	218.55	934.70	563.62	218.55	934.70	564.00	218.66
24	901.21	541.78	223.76	901.21	538.96	223.76	901.21	539.43	223.76
25	867.00	525.88	226.43	867.00	522.61	226.43	867.00	523.11	226.43
26	834.73	508.82	220.12	831.73		220.12	831.73	507.06	220.60
27	795.66	490.1	213.42	795.66		213.42	795.66		214.27
28	768.28	471.71	202.36	768.28		202.36	769.01		203.11
29	749.54	451.97	187.06	749.54		187.06	720.37		188.23
30	679.49			679.49			680.27		

$\Delta_1 F(K)$ is calculated from experimental data and then B_v and D_v are graphically determined by drawing $\Delta_1 F(K)/K^2$ as a function of K^2 .

B_e and α in equation $E_v = B_e - \omega(v+1/2)$ are also calculated and ω_e is obtained from Kratzer's relation. All constants are compiled in Table 3.

Table 3.

Elektron stufe	v	B	D	F	B_e	α	ω_e	r_e
${}^3\Pi$	0	16,29	$-1.72 \cdot 10^{-3}$	$5 \cdot 10^{-8}$	16,65	0,72	~ 8300	$1,04 \cdot 10^{-6}$
	1	15,57	$-1,77 \cdot 10^{-3}$	$5 \cdot 10^{-8}$				
${}^3\Sigma$	0	16,83	$-1,67 \cdot 10^{-3}$	$9 \cdot 10^{-8}$	16,65	0,64	~ 8300	
	1	15,19	$-1,65 \cdot 10^{-3}$	$8 \cdot 10^{-8}$				

The normal stage

We use the same term representation as in ${}^3\Pi$. The best constant values are here also obtained by using F_2 ; since we do not have a Λ splitting for which a mean value has to be calculated, we now start with the differences

$$\begin{aligned} R_2(K-1) - P_2(K+1) &= \Delta_2 F_2 = F_2(K+1) - F_2(K-1) \\ &= 4 B_v(K+\frac{1}{2}) + 8 D_v(K+\frac{1}{2})^3 - 12 F_v(K+\frac{1}{2})^5 \end{aligned}$$

and calculate the constants graphically.

Spin splitting

The existence of a marked spin splitting in ${}^3\Sigma$ levels can be seen from Table 4; it shows that $\Delta_2 F_2''(K) > \Delta_2 F_1''(K) > \Delta_2 F_3''(K)$. The process of /793 this splitting cannot be obtained by exclusively using the main branches for the calculation. We can, however, form ${}^3Q_{21}(K) - R_2(K)$ and ${}^3Q_{31}(K) - P_2(K)$ and then get $F_2 - F_1$ or $F_2 - F_3$. As can be seen from Table 5, $F_2 - F_1$ increases and $F_2 - F_3$ decreases as K increases. No more exact values can be expected considering that the lines are very weak, lying close to very strong ones and dispersion was rather small as mentioned above.

Table 4

K	$R_1(K-1)$ $-P_1(K+1)$	$R_2(K-1)$ $-P_2(K+1)$	$R_3(K-1)$ $-P_3(K+1)$	K	$R_1(K-1)$ $-P_1(K+1)$	$R_2(K-1)$ $-P_2(K+1)$	$R_3(K-1)$ $-P_3(K+1)$
8	293.18	292.90	292.72	16	1019.15	1019.05	1018.89
4	357.37	357.18	357.15	17	1073.21	1073.26	1073.10
5	421.18	421.10	420.86	18	1126.15	1126.09	1125.98
6	484.54	484.47	484.36	19	1177.58	1177.59	1177.52
7	547.87	547.25	547.08	20	1227.72	1227.66	1227.51
8	609.51	609.37	609.26	21	1276.88	1276.19	1276.19
9	670.81	670.76	670.64	22	1323.45	1323.24	1323.24
10	731.38	731.19	731.10	23	1386.95	1386.85	1386.95
11	791.04	790.83	790.86	24	1412.96	1412.96	1412.96
12	849.61	849.55	849.46	25	1455.28	1455.25	1455.28
13	907.24	907.11	907.08	26	1496.03	1496.03	1496.03
14	963.70	963.69	963.60	27	1534.98	1534.95	1534.98

Table 5

$$RQ_{11}(K) - R_1(K), \quad PQ_{12}(K) - P_1(K).$$

K	$F_2 - F_1$	$F_3 - F_2$	K	$F_2 - F_1$	$F_3 - F_2$
7	1.13	1.13	10	1.19	1.03
8	1.23	1.22	11	1.35	1.27
9	1.21	1.01	12		1.00

Table 6. The odd term values for $^3\Sigma$, if $F(K = 3) = 0$

K	F_3	F_2	F_1	$F_3 - F_2$	$F_2 - F_1$
3	0	0	0		
5	293.15	292.90	292.72	0.28	0.18
7	714.36	714.00	713.58	0.36	0.42
9	1261.73	1261.25	1260.66	0.48	0.59
11	1932.54	1932.01	1931.30	0.53	0.71
13	2723.58	2722.84	2722.16	0.71	0.68
15	3629.52	3629.95	3629.24	0.67	0.71
17	4649.97	4649.03	4648.13	0.94	0.90
19	5776.12	5775.12	5774.11	1.00	1.01
21	7006.54	7002.78	7001.62	1.06	1.16
23	8327.29	8326.02	8324.56	1.27	1.16
25	9740.25	9738.98	9737.52	1.27	1.16
27	11236.28	11235.01	11233.83	1.27	1.16

It can be seen from the Table that $F_2 - F_1 = F_2 - F_3$ at $K = 7$ or 8 , i.e., we can assume that $F_1 = F_3$ at $K = 7$ 1/2. We can subsequently obtain the second term value for F_3 , F_2 and F_1 by substituting $F_3(3) = 0$, $F_2(3) = 0$ and $F_1(3) = 0$ (see Table 6). We then form the differences $F_3(K) - F_2(K)$ and $F_2(K) - F_1(K)$ and draw a diagram of the changes of these differences with K . F_2 will be in the abscissa of this diagram, above it will be F_3 and below it F_1 . Lastly we shift the

curves for F_1 and F_3 parallel to themselves so that $K = 7$, $F_1 = F_3 = 1.18$. It can be seen that the differences in Table 5 which were obtained with the satellites fit well into the curve; it has furthermore the general appearance postulated by Kramer's theory and it is in accordance with the respective curves for O_2 and PH.

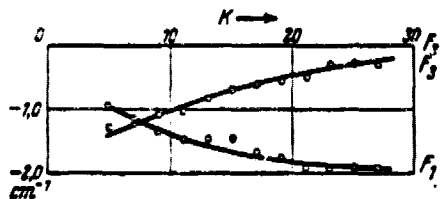


Fig. 32. Spin splitting in $^3\Sigma$; $v=0$

the most and does not change their general appearance.

It must be stressed, however, that there can be some uncertainty about the position of the point of intersection of the F_1 and F_3 curves, due to the fact that the few lines of the satellites are analyzed correctly; an error of this kind, however, effects a parallel shift of the curves at

A splitting

The material collected about A in 3II stages is rather insignificant and does not agree very well with the theories. In case a) it should be expected that the splitting in 3II_0 is large and independent of J, smaller for 3II_1 and proportional $J(J=1)$, and immeasurably small for 3II_2 . In case b) the splitting proportional to $K(K+1)$ and equal to 3II_0 , 3II_1 and 3II_2 should be expected since S is weakly coupled to A.

1795

Examples of A splitting are given by the first positive nitrogen group ⁴⁾ and PH ⁵⁾ for case a); both examples, however, do not follow the above-given diagram. The magnitude of the splitting is at least the one to be expected for N_2 . It is largest for 3II_0 , smaller for 3II_1 and smallest for 3II_2 . Not even this is true for PH.

⁴⁾ S.M. Naude. Proc. Roy. Soc. London (A) 136. 114. 1932.
⁵⁾ Loc.cit. Zeitschrift fuer Physik, Bd. 96

$^3\text{II}_0$ has the smallest splitting, both the other levels have a slightly larger one and about the same among themselves. For the study of this splitting, NH is better suited since it here is significantly larger than in both other molecules. It is largest for $^3\text{II}_1$, smaller for $^3\text{II}_2$ and smallest for $^3\text{II}_0$, the difference, however, is as postulated by theory, not exceptionally large. It could be concluded consequently that NH conforms better with theory than the earlier mentioned molecules. There are worse data, however, on the proportionality with $K(K+1)$. It is understandable that the curve follows a function $\Delta v_{ab} = c_1 + c_2 K + c_3 K^2 + \dots$, but since the meaning of these constants is unknown there is no use in calculating their values. The curves for $v=0$ and $v=1$ show a very similar shape and it can immediately be seen that the splitting is almost identical for $^3\text{II}_1$ and $^3\text{II}_2$ whereas the curve for $^3\text{II}_0$ is farther separated from the others, not to the extent, however, that it runs parallel to the curve for $^3\text{II}_1$.

1796
 A few other things should be mentioned. We here have an example for Δv_{ab} decreasing in its amount with increasing K , passing through zero and increasing again but with the opposite sign. Moving toward higher K values, however, the point is reached where the increase stops and splitting even starts to decrease again. The same effect could be noticed for BaH⁶⁾ for $^3\text{II}_{1,2}$ and in other molecules.

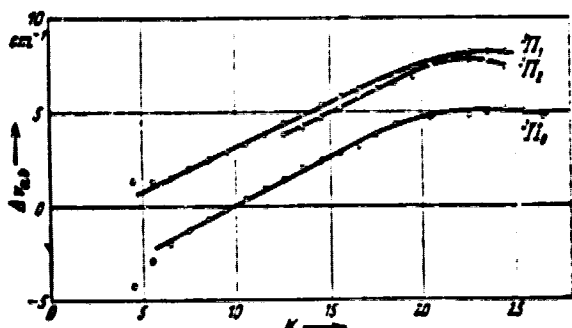
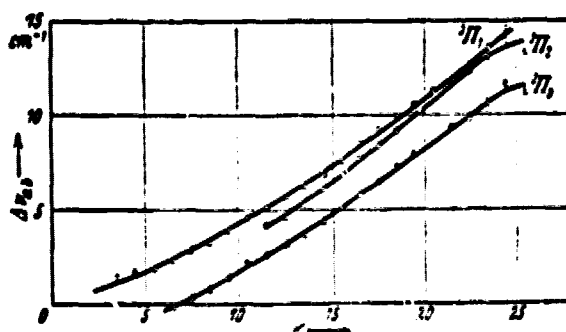


Fig. 3. A splitting in $^3\text{II}; v=0$

6) S.M. Naude, Proc. Roy. Soc. London (A) 136, 114. 1932

Fig. 4. A splitting in ^3II ; $v=1$

used. This widening effect, however, does not disappear totally when pressure is decreased, it is practically constant in the pressure range 100 to 1000 mm. The widening can consequently not exclusively be explained as pressure effect (Lorentz shock absorber or Stark effect of surrounding molecules), it must rather also have a pressure-independent cause like, e.g., the Doppler effect. Since it is not very worthwhile to study line widths in emission and especially in arcs with their hard to define relationships, no exact measurements of 3-db band widths were carried out. In their magnitude, however, they are about 0.04 \AA if pressure is lower than 1000 mm, and they seem to be the same for all lines.

For the Doppler effect the formula

$$\delta_w = \sqrt{\ln 2} \frac{\lambda}{c} \sqrt{\frac{2RT}{\mu}}$$

is valid and if temperature is roughly set to be 4000° , a Doppler effect of about 0.02 \AA is obtained. Consequently, the pressure independent widening of the lines can at least partly be regarded as due to Doppler effect. A light source like this one is actually not suited for maximum resolution of dense line accumulations, at

/797

The widening effect

As mentioned earlier, the recordings were made under rather high pressures so that the N_2 bands should disappear: this, however, caused an increased widening of the lines with increased pressure which became prominent because of the high dispersion

least not for light molecules since in this case the light source itself and not the optical instrument is setting the limit for resolution. Incidentally, the possibility exists that the Doppler effect is not alone responsible for the widening.

In order to better study these effects, experiments were carried out to obtain NH in absorption where all conditions like temperature, pressure etc. can be better determined. $^3\Sigma$ is an original state and absorption should be possible. The first experiments were carried out with a quartz spectrograph in a 1 m long iron tube heated to 750° by gas flames and filled with flowing ammonia gas. They were unsuccessful, however. Likewise no results yielded the experiments with a vacuum oven at different pressures and temperatures up to 1750° . N_2 and H_2 cannot be split and NH cannot be formed by increasing the temperature since the dissociation heat for N_2 is too high for an oven and besides it is higher than for NH, but it might be feasible that after decomposition of NH an intermediate product $NH + H_2$ or $NH + H + H$ is formed and that this might result in NH absorption. NH_3 decomposes readily at 900° ; the presence of NH is, however, not indicated by absorption at even this temperature.

As mentioned earlier, the NH spectrum is emitted by an illuminating gas flame, and the molecule consequently has to exist in it. An experiment was now arranged so that a 1.75 m long tube had slits which were cut out perpendicular to the longitudinal direction of the tube. A mixture of NH_3 and illuminating gas was introduced into the tube; this mixture flowed through the slits and then was lit so that a series of level flames was produced. Through them a parallel light beam from a tungsten lamp was sent toward a quartz spectrograph. A single, very diffuse absorption line at $\lambda 3360.14$ resulted. At $\lambda 3360.10$ lies the edge of Q_1 , and there is no doubt at all that it is this edge indeed. Since temperature is low in such a case, absorption of only the lowest energy levels can be expected. $R_1(0)$ and $R_2(0)$ start from level $K=0$; these lines, however, do not appear.

The Q lines must have the highest intensity, and since additionally many of them fall together in one point, it is not so strange that the Q edge should appear first. By this experiment is has consequently been confirmed that $^3\Sigma$ is the original state; more lines, however, should have been expected since -as shown above- the molecule is bound to be formed during ammonia decomposition and is thus also bound to absorb.

Lastly I would very much like to thank Prof. E. Hulthen, who initiated this study and who showed great interest in it. I thank Prof. Herzberg, Darmstadt for interesting discussions.

Stockholm, University Physics Institute, July 1935.